

PHYSICS

Timing of charge migration in betaine by impact of fast atomic ions

Patrick Rousseau^{1†}, Jesús González-Vázquez^{2,3†}, Dariusz G. Piekarski^{2‡}, Janina Kopyra⁴, Alicja Domaracka¹, Manuel Alcamí^{2,3,5}, Lamri Adoui¹, Bernd A. Huber¹, Sergio Díaz-Tendero^{2,3,6*}, Fernando Martín^{2,5,6*}

The way molecules break after ion bombardment is intimately related to the early electron dynamics generated in the system, in particular, charge (or electron) migration. We exploit the natural positive-negative charge splitting in the zwitterionic molecule betaine to selectively induce double electron removal from its negatively charged side by impact of fast O^{6+} ions. The loss of two electrons in this localized region of the molecular skeleton triggers a competition between direct Coulomb explosion and charge migration that is examined to obtain temporal information from ion-ion coincident measurements and nonadiabatic molecular dynamics calculations. We find a charge migration time, from one end of the molecule to the other, of approximately 20 to 40 femtoseconds. This migration time is longer than that observed in molecules irradiated by ultrashort light pulses and is the consequence of charge migration being driven by adiabatic nuclear dynamics in the ground state of the molecular dication.

INTRODUCTION

Understanding and controlling molecular damage induced by ionizing radiation, such as extreme ultraviolet (XUV) or x-ray light, fast electrons or ions, is one of the current challenges in natural sciences. It is well established that molecular damage can lead, among other processes, to random mutagenic miscoding or even lethal nanocoding of the DNA sequence, which is at the origin of several diseases (1–4). However, when conveniently controlled, ionizing irradiation can be the remedy rather than the problem, as demonstrated by current radio and hadron therapies (5, 6). An important source of damage is the environment surrounding the molecule, and, in this respect, several processes involving electron transfer between neighboring molecules have been proposed as electron transfer-mediated decay (ETMD) (7) or interatomic Coulombic decay (8). However, pioneering experimental and theoretical work (9, 10) has shown not only that molecular damage is also possible in isolated molecules but also that the nature of the resulting fragments is intimately related to the charge migration (CM) induced by the ionizing radiation at the very early stages, where most of the dynamics is governed by electronic motion. To experimentally investigate these early stages, one must first access the natural time scale of electronic motion, i.e., from several hundreds of attoseconds to a few femtoseconds, and then follow the ensuing coupled electron and nuclear dynamics within the next few tens of femtoseconds.

This is nowadays possible using XUV/x-ray attosecond and few femtosecond pulses produced either in the laboratory through high

harmonic generation or in large-scale x-ray free electron laser facilities, usually in the framework of pump-probe setups (11–16). The necessary time resolution is achieved using a short enough pump pulse, so that ionization is a “sudden” process in comparison with the subsequent CM process, which can then be probed using a second ultrashort pulse and varying the pump-probe delay with attosecond and few femtosecond resolution. In these experiments, CM results from the coherent superposition of electronic states created by the broadband pump pulse in the remaining molecular cation, and, therefore, it precedes nuclear motion (13, 16), although nuclear motion can have a notable effect at longer times (17, 18). In the case of x-ray pulses, the sudden ionization of the molecule can be followed by Auger decay, which can thus induce CM in the corresponding molecular dication (17, 19). One can also use ultrafast molecular dissociation associated to, e.g., proton emission or Coulomb explosion (CE) or both to clock the electron dynamics generated by the pump pulse. With the help of accurate theoretical calculations [see, e.g., (16, 20, 21) and references therein], the latter methods have been able to provide real-time pictures of electron dynamics in small- and medium-sized molecules ionized by infrared, XUV, and x-ray light (22–26).

CM induced by fast ions and electrons is, in general, very different from that induced by photons, as the latter usually involve less electronic channels as a result of selection rules. In addition, contrary to photons (and electrons), ions can selectively deposit energy in a well-localized region of a bulky target, as they can efficiently penetrate matter with low rates of diffusion and release most of their energy all at once just before stopping (the so-called Bragg peak) (27–29). So they are ideal, e.g., to treat tumors where extreme spatial localization is essential. Hence, understanding CM induced in collisions with atomic ions is not only important per se but also to explore new routes to trigger radiation damage by altering the early electron dynamics.

These studies require the implementation of specific experimental and theoretical approaches. In recent pump-probe experiments, ultrashort femtosecond pulses of electrons pioneered by Zewail and collaborators (30) have been successfully combined with ultrashort laser pulses with a time resolution of ~ 150 fs (31), which is comparable

Copyright © 2021
The Authors, some
rights reserved;
exclusive licensee
American Association
for the Advancement
of Science. No claim to
original U.S. Government
Works. Distributed
under a Creative
Commons Attribution
NonCommercial
License 4.0 (CC BY-NC).

¹Normandie Univ, ENSICAEN, UNICAEN, CEA, CNRS, CIMAP, 14000 Caen, France. ²Departamento de Química, Módulo 13, Universidad Autónoma de Madrid, 28049 Madrid, Spain. ³Institute for Advanced Research in Chemical Sciences (IAdChem), Universidad Autónoma de Madrid, 28049 Madrid, Spain. ⁴Faculty of Exact and Natural Sciences, Siedlce University of Natural Sciences and Humanities, 3 Maja 54, 08-110 Siedlce, Poland. ⁵Instituto Madrileño de Estudios Avanzados en Nanociencia (IMDEA Nano), Cantoblanco, 28049 Madrid, Spain. ⁶Condensed Matter Physics Center (IFIMAC), Universidad Autónoma de Madrid, 28049 Madrid, Spain.

*Corresponding author. Email: fernando.martin@uam.es (F.M.); sergio.diaztendero@uam.es (S.D.-T.)

†These authors contributed equally to this work.

‡Present address: Institute of Physical Chemistry, Polish Academy of Sciences, Kasprzaka 44/52, 01-224 Warsaw, Poland.

to that achieved in state-of-the-art femtochemistry experiments performed with lasers, but provide, in addition, spatial atomic resolution. In the case of atomic ions, this is not yet possible, mainly because of the difficulty to produce ultrashort pulsed ionic beams in conventional ion accelerators. This is despite the fact that an ion of approximately a few kilo-electron volt per atomic mass unit (keV/amu) interacts with a small- or medium-sized molecule for no more than a few femtoseconds (e.g., a 3 keV/amu projectile has a velocity of 7.6 Å/fs), which is the optimum scenario to induce a sudden ionization of the molecular target, hence to investigate CM processes in their natural time scale. To achieve the necessary few-femtosecond time resolution, in this work, we will use ultrafast CE as an internal clock of the electron dynamics generated by the ionizing collision. This is not always an available option, but, as we will see below, it can be achieved by a smart selection of the ionic projectile and molecular target.

Here, we exploit the natural positive-negative charge splitting in the betaine zwitterion (*N, N, N*-trimethylglycine; see Fig. 1C) to selectively induce double ionization on the negatively charged end of the molecule by impact of 3 keV/amu O^{6+} and then trigger a competition between direct CE and CM involving the two positively charged ends of the doubly ionized molecule. The analysis of the kinetic energy distributions of the resulting positively charged fragments detected in coincidence along with the results of *ab initio* nonadiabatic molecular dynamics simulations allows us to determine a CM time from

end to end of approximately 20 to 40 fs. The calculations also show that CM is mainly driven by nuclear motion in the ground state of the molecular dication, thus leading to migration times longer than those observed in CM triggered by electronic coherences (13, 16, 32).

RESULTS AND DISCUSSION

With a positive charge localized on the quaternary ammonium group [$-N^+(CH_3)_3$] and a negative charge on the carboxylate group [$-CO_2^-$] (see Fig. 1C), the (neutral) betaine molecule [$N(CH_3)_3-CH_2-COO$] has a rather large permanent dipole of 11.5 D [4.5 atomic units (a.u.)] (33). Figure 1 (A and B) shows the potential energy curves of the (O^{6+} -B) system (where B stands for betaine) for the case in which the O^{6+} projectile lies in the direction of the betaine permanent dipole μ (Fig. 1C). The orientation of the molecule is such that the charge-dipole interaction between the projectile (P) and the target (T) is the most attractive. The potential energy curves and the energy ranges associated with the single and double electron capture channels have been obtained using the experimental bound-state energies of O^{6+} , O^{5+} , and O^{4+} (34); the calculated energies of the autoionizing doubly excited states of O^{4+} (35); the calculated first, second, and third vertical ionization potentials of betaine (see Methods for details); and the asymptotic analytical formulas that describe the repulsive charge-charge, $q_P q_T/d$, and attractive charge-dipole, $q_P(\mu \cdot \mathbf{d})/d^3$, interactions between the different projectile and target species, where d is the distance between the projectile and the center of mass of the target (36). The latter formulas are expected to accurately represent the actual behavior of the potential energy curves except at very short projectile-target distances, where electron delocalization over the projectile and the target can be important. As can be seen, the potential energy curve of the entrance channel O^{6+} -B intersects the repulsive curves of the $O^{4+}(1s^2 3l n l')-B^{2+}$ channels, associated with double electron capture, at projectile-target distances between 5 and ~ 10 a.u., where nonadiabatic transitions from the former to the latter channels should be very efficient at the impact energy considered in this work (37). The same applies to the $O^{5+}(1s^2 3l)-B^+$ and $O^{5+}(1s^2 4l)-B^+$ channels, associated with single electron capture, which appear in the same energy region as the double electron capture channels. Therefore, one can expect that both single and double electron capture (either direct or mediated by single electron capture channels) will be very efficient processes. These are also expected to occur, although to a lesser extent, when the molecule is oriented at 90° with respect to the incidence direction, as $\mu \cdot \mathbf{d} = 0$ and the corresponding potential energy curve mostly coincides with the zero-energy axis. This curve crosses single and double electron capture channels in a similar range of projectile-target distances, although involving slightly higher n and l quantum numbers in the projectile side, which are less favorable because of the large number of radial and angular nodes in the corresponding wave functions [Barat-Lichten rules (38)]. If the orientation of the betaine molecule was reversed with respect to the first one, then the potential energy curve of the entrance channel would be the mirror image of that shown in Fig. 1 (A and B) with respect to the zero-energy axis, i.e., it would be entirely repulsive and therefore would not lead to substantial single and double electron capture in the above mentioned channels. That is, the charge-dipole interaction that governs the approach of the projectile to the target and the orientation selectivity of the double-electron capture process restrict the range of molecular orientations where doubly charged betaine can be formed. We can safely discard

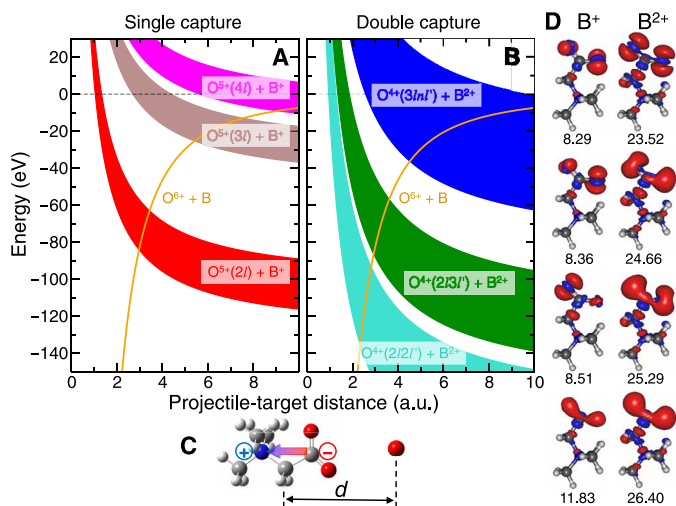


Fig. 1. The O^{6+} -betaine system. Molecular energies for (A) single electron capture and (B) double electron capture channels as a function of the distance between the O^{6+} projectile and the center of mass of the betaine molecule oriented as shown in (C). For the sake of clarity, only the energy ranges covered by the single and double electron capture channels leading to $O^{5+}(nl)$ with $n < 5$ (A) and $O^{4+}(2lnl')$ with $n < 4$ and $O^{4+}(3lnl')$ (B) are shown. The missing channels are expected to be barely populated in the collision or lie outside the axes range. Notice that the incoming projectile approaches the molecule from the side of the negatively charged carboxylate group, which is the most favorable orientation for single and double electron capture (see main text). The orange curves in (A) and (B) represent the entrance channel. The electron densities, referred to the ground-state electron density of neutral betaine, for the lowest states of singly and doubly charged betaine resulting from single and double electron capture, respectively, are shown in (D). The numbers below the density maps indicate the energies (in electron volts) of the corresponding electronic states of singly and doubly charged betaine with respect to the energy of the ground state of neutral betaine.

ionization as a possible source of doubly charged betaine, because, for the impact energy considered in our work (3 keV/amu), the ionization cross section is several orders of magnitude smaller than that associated with electron capture [see, e.g., (39, 40) for the case of proton-hydrogen and proton-uracil collisions]. For the same reason, transfer ionization and ETMD (7, 41), in which a betaine electron directly goes into the continuum (ionization) and another betaine electron is transferred to the projectile (capture), thus leading to a betaine dication, are expected to be less likely than two resonant electron transfers to the projectile (39, 40, 42). Last, two electron processes implying the removal of electrons from inner shells (non-resonant electron capture) can also be discarded, because target inner vacancy states lie very far in energy from the entrance channel (these states lie out of scale in Fig. 1).

Figure 1D shows the electron density of the four lowest states of singly and doubly ionized betaine referred to the ground-state density of neutral betaine. As can be seen, the removal of one or two electrons always involves the $-\text{CO}_2^-$ side of the zwitterion, meaning that, after double electron capture (either direct or sequential), this side of the molecule will hold a positive charge, while the charge distribution in the rest of the molecule will basically remain unchanged. This fact, combined with the high preference for the molecular orientation shown in Fig. 1C, indicates a high selectivity of the double electron capture process, which basically leads to a doubly charged betaine molecule with a positively charged $-\text{CO}_2^+$ side and a positively charged $-\text{N}(\text{CH}_3)_3^+$ side, well separated from each other. These are the optimal conditions for a clean and rapid CE of B^{2+} , which is expected to compete with internal CM, where an electron would move from the $-\text{N}(\text{CH}_3)_3^+$ side to the $-\text{CO}_2^+$ high electron affinity side, thus neutralizing the positive charge in the latter side. The two competing processes are expected to lead to different

molecular fragments, as illustrated in Fig. 2A: CE can lead to CO_2^+ and other molecular fragments, while CM is not expected to lead to any CO_2^+ .

To confirm this picture, we have performed ion-ion coincident measurements of the ionic fragments produced in collisions of 3 keV/amu O^{6+} with fully deuterated betaine. We have chosen deuterated betaine to unambiguously assign fragments using time-of-flight (TOF) mass spectrometry [e.g., both $\text{N}(\text{CH}_3)_2^+$ and CO_2^+ have mass/charge ratio (m/z) = 44, while $\text{N}(\text{CD}_3)_2^+$ has m/z = 50]. Figure 2 (B and C) shows zooms in regions of the ion-ion coincidence map around the $(m_1/z_1)^+/(m_2/z_2)^+$ islands $18^+/66^+$ and $44^+/66^+$, corresponding to, respectively, $\text{CD}_3^+ / (\text{CD}_2)\text{N}(\text{CD}_3)_2^+$ and $\text{CO}_2^+ / (\text{CD}_2)\text{N}(\text{CD}_3)_2^+$ coincidences. The full ion-pair coincidence map is given in the Supplementary Materials. The $44^+/66^+$ island arises from direct CE of doubly charged betaine into $\text{CO}_2^+ / (\text{CD}_2)\text{N}(\text{CD}_3)_2^+$ and the subsequent emission of a neutral methyl group (CD_3) from the larger fragment, thus leading to $\text{CO}_2^+ / (\text{CD}_2)\text{N}(\text{CD}_3)_2^+ / \text{CD}_3$. This two-step mechanism is confirmed by the slope of the $44^+/66^+$ island, which is approximately $-66/(66 + 18)$, suggesting also that the neutral CD_3 fragment emitted in the second step has a negligible momentum [see (43, 44) for the connection between the slopes of coincident islands and n -body fragmentation].

The $18^+/66^+$ island is associated with three body fragmentation of doubly charged betaine after neutralization of the $-\text{CO}_2$ side by CM, leading to $\text{CO}_2 / \text{CD}_3^+ / (\text{CD}_2)\text{N}(\text{CD}_3)_2^+$. In this case, the slope of the coincidence island is positive and cannot be explained as resulting from a two-step process in which CE is followed by emission with negligible momentum of neutral CO_2 from one of the charged fragments, as this process would always lead to an island with negative slope. A positive slope indicates that the two charged fragments are emitted in the same direction (45), while neutral CO_2 is emitted

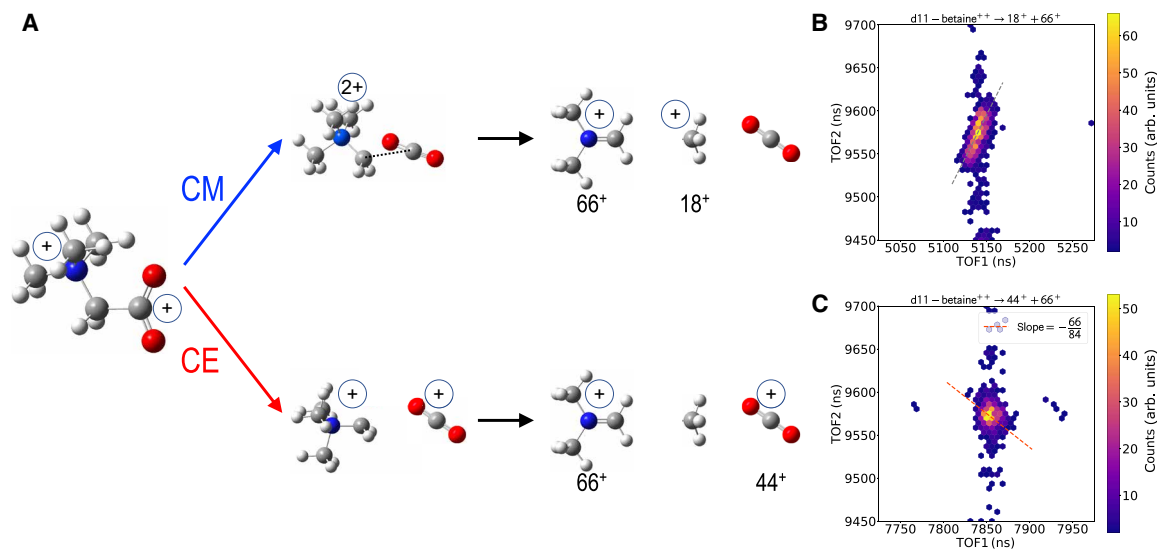


Fig. 2. Fragmentation of fully deuterated doubly charged betaine. (A) As a result of double electron capture by the projectile from the carboxylate group, both ends of the betaine molecule are positively charged. Two scenarios are then possible: direct CE and CM. In CE, charge separation by cleavage of the $\text{C}_{\text{carboxylate}}-\text{C}_\alpha$ bond leads to the two charged fragments CO_2^+ and $(\text{CD}_2)\text{N}(\text{CD}_3)_2^+$. The latter further dissociates by emission of a neutral methyl group CD_3 . Experimentally, this process leads to a coincidence $44^+/66^+$ in the ion-ion map (C). The slope of the measured island, given by momentum conservation, confirms this scheme (see main text). In contrast, after CM, the ammonium side of the betaine is doubly charged, so that the emission of a neutral carboxylate group CO_2 is expected and the ulterior charge separation gives rise to two charged fragments, CD_3^+ and $(\text{CD}_2)\text{N}(\text{CD}_3)_2^+$. Experimentally, one observes a coincidence island $18^+/66^+$ in the ion-ion map (B) with a positive slope, indicating that fragmentation involves the formation of the intermediate species shown in the top row of (A) (see main text).

with large momentum in the opposite direction to compensate the momentum of the charged particles. This picture is consistent with the formation of an intermediate doubly charged transient structure as that shown in the top panel of Fig. 2A, which, according to our calculations (see below), corresponds to a minimum in the potential energy surface arising from the attractive charge/induced-dipole interaction between $(\text{CD}_2)\text{N}(\text{CD}_3)_3^+$ and a neutral CO_2 fragment in the early stages of dissociation.

To get a deeper insight into the results of these measurements, we have performed few switches trajectory surface hopping calculations on the lowest potential energy surfaces of the betaine dication obtained within the complete active space perturbation theory (CASPT2) approach (see Methods for details). Figure 3 summarizes the most important results. Figure 3A shows the time evolution of the local charge around the CO_2 group for trajectories starting from the ground and first excited state of the betaine dication. As can be seen, within the limited time interval considered in our calculations (see the Supplementary Materials for an extension up to 150 fs), trajectories starting at the ground state can only lead to CO_2 charges equal to 0 or around +0.75, which are consistent with the charges that should be observed only after CM or in the intact betaine dication, respectively. In contrast, trajectories starting in the first excited state can only lead to CO_2 charges equal to +1 or around +0.75, compatible with CE and the intact betaine dication, respectively. Trajectories starting in the second excited state (not shown in the figure for the sake of clarity; see the Supplementary Materials) follow a similar pattern: They do not lead to neutral CO_2 . Figure 3A also shows that neutralization of the initial positive charge in the CO_2 site is completed in 20 to 40 fs while acquiring the +1 charge required for CE takes around 100 fs.

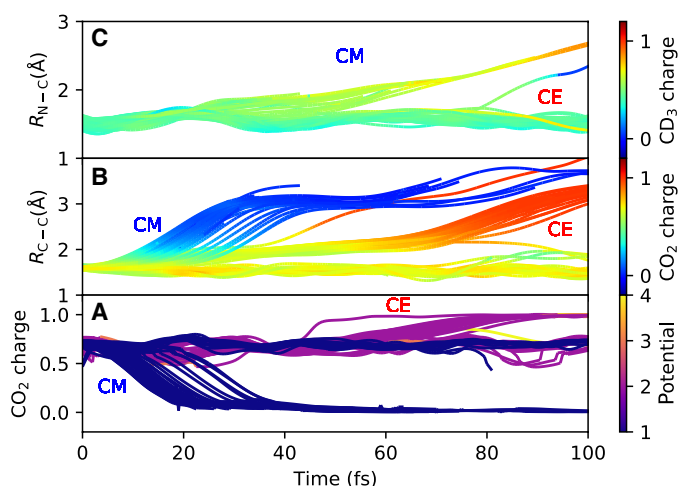


Fig. 3. Molecular dynamics calculations. (A) Evolution of the charge located at the CO_2 end of doubly charged betaine for all trajectories starting in the ground (i) and the first excited (ii) state. The color palette on the right indicates the potential energy surface in which the trajectory evolves at every time. Notice that a significant number of trajectories starting in the ground state lead to neutralization of the CO_2 end. (B) Evolution of the $\text{C}_{\text{carboxylate}}-\text{C}_{\alpha}$ bond distance in doubly charged betaine for all trajectories starting in the ground and the first excited state. The color palette on the right indicates the charge in the CO_2 end at every time. Notice that the $\text{C}_{\text{carboxylate}}-\text{C}_{\alpha}$ bond breaks faster in CM than in CE. (C) Evolution of the $\text{N}-\text{C}$ bond distance in doubly charged betaine for all trajectories starting in the ground and the first excited state. The color palette on the right indicates the charge in the CD_3 site at every time.

Figure 3 (B and C) shows that the times needed by CO_2 to acquire its final charge strongly correlate with the times needed by the charged molecular fragments to complete the dissociation process. As can be seen in Fig. 3B, when CO_2 becomes completely neutral after 20 to 40 fs, the $\text{C}-\text{C}$ distance has increased by more than 1 Å (i.e., more than 2 a.u.), while it remains almost unchanged for those trajectories leading to a charge +1 in the CO_2 side. In the latter case, a variation of 1 Å in the $\text{C}-\text{C}$ distance is only observed after approximately 100 fs, showing that acquiring the right +1 charge and fragmenting are concerted processes. CD_3^+ fragments associated with CM acquire their final +1 charge in about 100 fs (see Fig. 3C), while, in the case of CE, the CD_3 sites preserve their initial charge at all times. The $\text{C}-\text{C}$ distance remains more or less constant for around 20 fs after neutralization of the CO_2 ends (Fig. 3B) but, with no exception, emission of neutral CO_2 is irreversibly produced at later times. The existence of such a plateau in the $\text{C}-\text{C}$ distance is due to the transient formation of the doubly charged complex depicted in Fig. 2A, which delays for about 20 fs of the ejection of neutral CO_2 and the ensuing fragmentation of the remaining dication into $\text{CD}_3^+ / (\text{CD}_2)\text{N}(\text{CD}_3)_2^+$. This result is compatible with the observation of a positive slope in the $18^+/66^+$ island, since the fact that CO_2 leaves first makes the two charged fragments go in the same direction (i.e., opposite to the CO_2 emission direction).

The results given in Fig. 3 show that CM is mostly an adiabatic process taking place in the ground state of the betaine dication. This interpretation is confirmed by the absence of avoided crossings between the ground and the excited electronic states of doubly charged betaine and the conservation of the ground-state electronic character along the minimum energy path leading to emission of neutral CO_2 (see the Supplementary Materials). So, CM is almost entirely driven by nuclear motion in this ground state, which explains why CM in doubly charged betaine is substantially slower than charge fluctuations resulting exclusively from electronic coherences induced by ionizing radiation, e.g., using attosecond and few-femtosecond laser or electron pulses.

An analysis of the kinetic energy release (KER) of the $\text{CD}_3^+ / (\text{CD}_2)\text{N}(\text{CD}_3)_2^+$ and $\text{CO}_2^+ / (\text{CD}_2)\text{N}(\text{CD}_3)_2^+$ ion pairs associated with, respectively, the $18^+/66^+$ and $44^+/66^+$ peaks observed in the ion-ion coincidence spectrum confirms the general trends resulting from our calculations. The details of this analysis are given in Methods and the Supplementary Materials. The KERs are shown in Fig. 4 (A and B), respectively, in the form of histograms. Both distributions peak at zero kinetic energy and decrease with energy. However, the KER associated with CE [i.e., the $\text{CO}_2^+ / (\text{CD}_2)\text{N}(\text{CD}_3)_2^+$ coincidence] is substantially narrower, indicating that CE (or, equivalently, emission of CO_2^+) is slower than the fragmentation into $\text{CD}_3^+ / (\text{CD}_2)\text{N}(\text{CD}_3)_2^+$ that follows CM (see Fig. 2A). This fact can be more clearly seen in Fig. 4, C and D, where the corresponding KER histograms have been converted into time histograms by assuming that direct CE and CD_3^+ emission following CM are practically irreversible when the two charged fragments have traveled a distance of 2 a.u. from their initial positions. As can be seen, for CM, the time histogram peaks at around 50 fs, whereas, for CE, approximately 90% of the events take much longer than 50 fs in excellent agreement with our theoretical findings, in particular with our estimation of the CM time. The time histogram for direct CE given in Fig. 4D shows an increase in the number of events at around 50 fs, which is more or less the time taken by CM to occur. When direct CE is that fast, one can expect that it efficiently competes with CM, thus highlighting the effect of possible

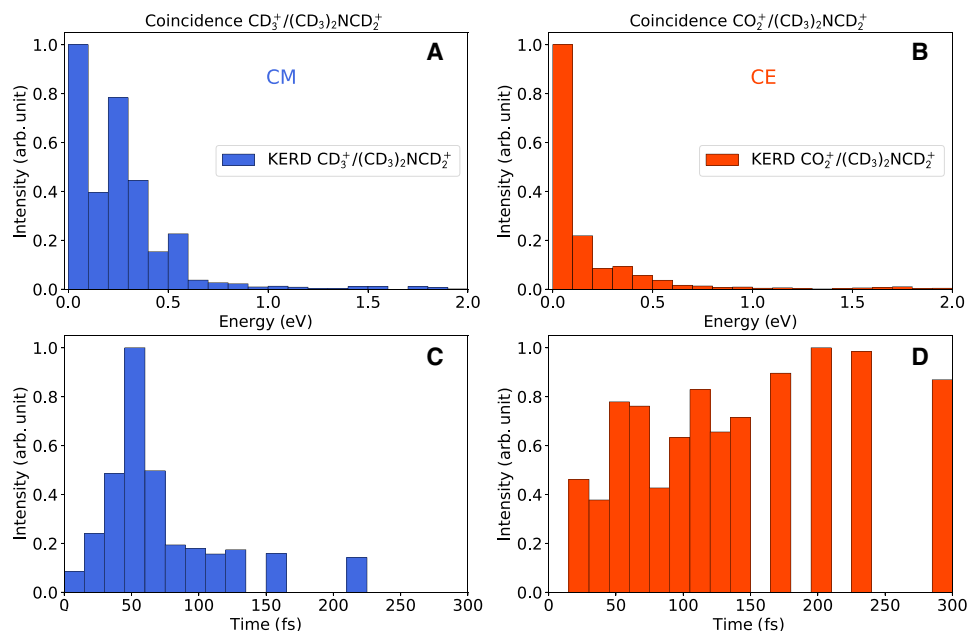


Fig. 4. KER and estimation of the charge separation time. KER for (A) CD₃⁺ fragments detected in coincidence with 66⁺ fragments (associated with CM) and (B) CO₂⁺ fragments detected in coincidence with 66⁺ fragments (associated with direct CE). (C and D) Estimation of the time necessary for the separation of the two charges leading to the corresponding ion pairs 18⁺/66⁺ and 44⁺/66⁺ based on their respective KER distribution (KERD).

electronic coherences between the CE and CM channels. Since determination of the kinetic energy of the fragments from the measured TOF distribution is not as accurate as that provided by position sensitive detectors, further experimental work allowing for the direct measurement of fragments momentum could shed more light on this issue and probably allow for a more accurate retrieval of the CM time from experiment by focusing on the KER region where interferences between CE and CM channels are expected to occur.

Taking advantage of the natural positive-negative charge separation in the betaine zwitterion, we have been able to selectively induce double electron removal from the negatively charged end of the molecule in collisions with 3 keV/amu O⁶⁺ ions. This process initiates a competition between direct CE and CM that can be used to obtain temporal information about the several stages involved in these processes. We have determined an internal CM time, from one end of the molecule to the other, of approximately 20 to 40 fs and show that this process preferentially takes place in the ground state of the betaine dication resulting from the collision, while direct CE mainly occurs in its excited states. The CM time is substantially longer than that previously observed in charge dynamics induced by electronic coherences in molecules of similar complexity. This is the consequence of CM being mostly driven by adiabatic nuclear dynamics in the ground state of the betaine dication.

METHODS

Experiment

The experiments have been performed at ARIBE (46), the low-energy ion beam facility of Grand Accélérateur National d'Ions Lourds (GANIL, Caen, France). The experimental setup and methods have been described in detail elsewhere (47). Briefly, the O⁶⁺ ions are produced in an electron cyclotron resonance ion source, accelerated at 48 keV, and mass-analyzed by a magnet sector. The beam is pulsed in

bunches of 500 ns and transported by ion optics toward the crossed-beam collision device where, after focusing, it interacts with an effusive beam of neutral betaine molecules produced by evaporation of a commercial sample of fully deuterated betaine (purity 98%; Eurisotop) in a heated oven. Just after the passage of the ion bunch, the cationic products of the interaction are extracted by a pulsed electric field into a modified Wiley-McLaren TOF mass spectrometer (48). Their arrival times are recorded in an event-by-event mode allowing us to consider coincidences among them (49, 50). The KER of an ion pair is obtained after differentiation of the distribution of the time difference between two fragments (51, 52). SIMION simulations of the TOF spectrometer show that the ion transmission is 100% for cations with a kinetic energy up to 10 eV (53). From the relative velocity of the two fragments, one can estimate the time required to run a given distance.

Theory

Optimized geometry and frequencies for the betaine molecule were obtained in the ground electronic state using the Møller-Plesset (MP2) method with the cc-pvDZ-jkfit basis (54) as implemented in the Brilliantly Advanced General Electronic-structure Library (BAGEL) code (55). Starting from this geometry, a set of 50 initial conditions was obtained using a harmonic Wigner distribution of correlated position and momentum. To describe the electronic states of the different ionization states of betaine, single-point state-average complete active space self-consistent field calculations were performed for the neutral (singlet), cation (doublet), dication (singlet and triplet), and trication (doublet) at the MP2 geometry using a state average of four electronic states, without symmetry considerations, with an active space consisting of 9 orbitals and 10 electrons for the dication. To simulate the nonadiabatic semiclassical dynamics, a local version of the SHARC (57) method was used. The electronic structure was represented, including gradients, at the XMS-CASPT2 level

(58) with an imaginary shift of 0.2 a.u. using the BAGEL code (55). For the calculation of the nonadiabatic couplings, the overlap matrix between two consecutive time steps was used. For this, the perturbed modified wave function, including configuration interaction vectors and molecular orbitals, was extracted from BAGEL (55) and imported into the OpenMolcas code (56) with overlaps obtained with the RASSI program. Charges on different molecular sites were evaluated by performing a Mulliken analysis.

SUPPLEMENTARY MATERIALS

Supplementary material for this article is available at <https://science.org/doi/10.1126/sciadv.abg9080>

REFERENCES AND NOTES

- B. Boudaïffa, P. Boudaïffa, D. Hunting, M. A. Huels, L. Sanche, Resonant formation of DNA strand breaks by low-energy (3 to 20 eV) electrons. *Science* **287**, 1658–1660 (2000).
- C. E. Crespo-Hernández, B. Cohen, P. M. Hare, B. Kohler, Ultrafast excited-state dynamics in nucleic acids. *Chem. Rev.* **104**, 1977–2020 (2004).
- W. Siede, Y. W. Kowband, P. W. Doetsch, *DNA Damage Recognition* (Taylor & Francis, 2006).
- R. P. Sinha, D.-P. Häder, UV-induced DNA damage and repair: A review. *Photochem. Photobiol. Sci.* **1**, 225–236 (2002).
- V. T. DeVita Jr., T. S. Lawrence, S. A. Rosenberg, *Principles of Radiation Oncology in Cancer* (Lippincott Williams and Wilkins, 2008).
- M. Durante, J. S. Loeffler, Charged particles in radiation oncology. *Nat. Rev. Clin. Oncol.* **7**, 37–43 (2010).
- V. Stumpf, K. Gokhberg, L. S. Cederbaum, The role of metal ions in x-ray-induced photochemistry. *Nat. Chem.* **8**, 237–241 (2016).
- L. S. Cederbaum, J. Zobeley, F. Tarantelli, Giant intermolecular decay and fragmentation of clusters. *Phys. Rev. Lett.* **79**, 4778–4781 (1997).
- R. Weinkauff, P. Schanen, D. Yang, S. Soukara, E. W. Schlag, Elementary processes in peptides: Electron mobility and dissociation in peptide cations in the gas phase. *J. Phys. Chem.* **99**, 11255–11265 (1995).
- R. Weinkauff, E. W. Schlag, T. J. Martinez, R. D. Levine, Nonstationary electronic states and site-selective reactivity. *Chem. Eur. J.* **101**, 7702–7710 (1997).
- G. Sansone, F. Kelkensberg, J. F. Pérez-Torres, F. Morales, M. F. Kling, W. Siu, O. Ghafur, P. S. Jonsson, M. Swoboda, E. Benedetti, F. Ferrari, F. Lépine, J. L. Sanz-Vicario, S. Zherebtsov, I. Znakovskaya, A. L'Huillier, M. Y. Ivanov, M. Nisoli, F. Martín, M. J. J. Vrakking, Electron localization following attosecond molecular photoionization. *Nature* **465**, 763–766 (2010).
- L. Belshaw, F. Calegari, M. J. Duffy, A. Trabattani, L. Poletto, M. Nisoli, J. B. Greenwood, Observation of ultrafast charge migration in an amino acid. *J. Phys. Chem. Lett.* **3**, 3751–3754 (2012).
- F. Calegari, D. Ayuso, A. Trabattani, L. Belshaw, S. de Camillis, S. Anumula, F. Frassetto, L. Poletto, A. Palacios, P. Decleva, J. B. Greenwood, F. Martín, M. Nisoli, Ultrafast electron dynamics in phenylalanine initiated by attosecond pulses. *Science* **346**, 336–339 (2014).
- P. Ranitovic, C. W. Hogle, P. Riviere, A. Palacios, X. M. Tong, N. Toshima, A. Gonzalez-Castrillo, L. Martin, F. Martin, M. M. Murnane, H. Kapteyn, Attosecond vacuum UV coherent control of molecular dynamics. *Proc. Natl. Acad. Sci.* **111**, 912–917 (2014).
- A. Marciniak, V. Despré, V. Lorient, G. Karras, M. Hervé, L. Quintard, F. Catoire, C. Joblin, E. Constant, A. I. Kuleff, F. Lépine, Electron correlation driven non-adiabatic relaxation in molecules excited by an ultrashort extreme ultraviolet pulse. *Nat. Commun.* **10**, 337 (2019).
- M. Nisoli, P. Decleva, F. Calegari, A. Palacios, F. Martín, Attosecond electron dynamics in molecules. *Chem. Rev.* **117**, 10760–10825 (2017).
- C. Arnold, O. Vendrell, R. Santra, Electronic decoherence following photoionization: Full quantum-dynamical treatment of the influence of nuclear motion. *Phys. Rev. A* **95**, 033425 (2017).
- J. Delgado, M. Lara-Astiaso, J. González-Vázquez, P. Decleva, A. Palacios, F. Martín, Molecular fragmentation as a way to reveal early electron dynamics induced by attosecond pulses. *Faraday Discuss.* **228**, 349–377 (2021).
- A. Picón, C. Bostedt, C. Hernández-García, L. Plaja, Auger-induced charge migration. *Phys. Rev. A* **98**, 043433 (2018).
- A. I. Kuleff, L. S. Cederbaum, Ultrafast correlation-driven electron dynamics. *J. Phys. B Atomic Mol. Phys.* **47**, 124002 (2014).
- M. Kowalewski, B. P. Fingerhut, K. E. Dorfman, K. Bennett, S. Mukamel, Simulating coherent multidimensional spectroscopy of nonadiabatic molecular processes: From the infrared to the x-ray regime. *Chem. Rev.* **117**, 12165–12226 (2017).
- M. Pitzer, M. Kunitski, A. S. Johnson, T. Jahnke, H. Sann, F. Sturm, L. P. H. Schmidt, H. Schmidt-Böcking, R. Dörner, J. Stohner, J. Kiedrowski, M. Reggelin, S. Marquardt, A. Schießer, R. Berger, M. S. Schöffler, Direct determination of absolute molecular stereochemistry in gas phase by Coulomb explosion imaging. *Science* **341**, 1096–1100 (2013).
- A. Rudenko, L. Inhester, K. Hanasaki, X. Li, S. J. Robatjazi, B. Erk, R. Boll, K. Toyota, Y. Hao, O. Vendrell, C. Bomme, E. Savelyev, B. Rudek, L. Foucar, S. H. Southworth, C. S. Lehmann, B. Kraessig, T. Marchenko, M. Simon, K. Ueda, K. R. Ferguson, M. Bucher, T. Gorkhova, S. Carron, R. Alonso-Mori, J. E. Koglin, J. Correa, G. J. Williams, S. Boutet, L. Young, C. Bostedt, S. K. Son, R. Santra, D. Rolles, Femtosecond response of polyatomic molecules to ultra-intense hard x-rays. *Nature* **546**, 129–132 (2017).
- T. Yatsushashi, N. Nakashima, Multiple ionization and Coulomb explosion of molecules, molecular complexes, clusters and solid surfaces. *J. Photochem. Photobiol. C Photochem. Rev.* **34**, 52–84 (2018).
- F. Allum, M. Burt, K. Amini, R. Boll, H. Köckert, P. K. Olshin, S. Bari, C. Bomme, F. Brauße, B. C. de Miranda, S. Düsterer, B. Erk, M. Géléoc, R. Geneaux, A. S. Gentleman, G. Goldshtein, R. Guillemin, D. M. P. Holland, I. Ismail, P. Johnsson, L. Journal, J. Küpper, J. Lahl, J. W. L. Lee, S. Maclot, S. R. Mackenzie, B. Manschwetus, A. S. Mereshchenko, R. Mason, J. Palaudoux, M. N. Piancastelli, F. Penet, D. Rompotis, A. Rouzée, T. Ruchon, A. Rudenko, E. Savelyev, M. Simon, N. Schirmel, H. Stapelfeldt, S. Teichert, O. Travnikova, S. Trippel, J. G. Underwood, C. Vallance, J. Wiese, F. Ziaee, M. Brouard, T. Marchenko, D. Rolles, Coulomb explosion imaging of CH₃I and CH₂ClI photodissociation dynamics. *J. Chem. Phys.* **149**, 204313 (2018).
- R. Y. Bello, S. E. Canton, D. Jelovina, J. D. Bozek, B. Rude, O. Smirnova, M. Y. Ivanov, A. Palacios, F. Martín, Reconstruction of the time-dependent electronic wave packet arising from molecular autoionization. *Sci. Adv.* **4**, eaa3962 (2018).
- U. Amaldi, G. Kraft, Radiotherapy with beams of carbon ions. *Rep. Prog. Phys.* **68**, 1861–1882 (2005).
- D. Kramer, Carbon-ion cancer therapy shows promise. *Phys. Today* **68**, 24 (2015).
- D. Schulz-Ertner, H. Tsujii, Particle radiation therapy using proton and heavier ion beams. *J. Clin. Oncol.* **25**, 953–964 (2007).
- J. C. Williamson, J. Cao, H. Ihee, H. Frey, A. H. Zewail, Clocking transient chemical changes by ultrafast electron diffraction. *Nature* **386**, 159–162 (1997).
- J. Yang, X. Zhu, J. P. F. Nunes, J. K. Yu, R. M. Parrish, T. J. A. Wolf, M. Centurion, M. Gühr, R. Li, Y. Liu, B. Moore, M. Niebuhr, S. Park, X. Shen, S. Weathersby, T. Weinacht, T. J. Martinez, X. Wang, Simultaneous observation of nuclear and electronic dynamics by ultrafast electron diffraction. *Science* **368**, 885–889 (2020).
- M. Lara-Astiaso, M. Galli, A. Trabattani, A. Palacios, D. Ayuso, F. Frassetto, L. Poletto, S. de Camillis, J. Greenwood, P. Decleva, I. Tavernelli, F. Calegari, M. Nisoli, F. Martín, Attosecond pump-probe spectroscopy of charge dynamics in tryptophan. *J. Phys. Chem. Lett.* **9**, 4570–4577 (2018).
- J. Rak, P. Skurski, M. Gutowski, An ab initio study of the betaine anion–dipole-bound anionic state of a model zwitterion system. *J. Chem. Phys.* **114**, 10673–10681 (2001).
- NIST Atomic Spectra Database, National Institute of Standards and Technology, Gaithersburg, MD (2018); <https://physics.nist.gov/asd>.
- H. Bachau, P. Galan, F. Martin, A. Riera, M. Yáñez, Resonance parameters and properties of beryllium-like doubly excited states: $4 \leq z \leq 10$. *At. Data Nucl. Data Tables* **44**, 305–348 (1990).
- Karplus, M., Porter, R. H. *Atoms and Molecules: An Introduction for Students of Physical Chemistry* (W. A. Benjamin, 1970); <http://openlibrary.org/books/OL5313877M>.
- A. Macías, A. Riera, Ab initio quantum chemistry in the molecular model of atomic collisions. *Phys. Rep.* **90**, 299–376 (1982).
- M. Barat, W. Lichten, Extension of the electron-promotion model to asymmetric atomic collisions. *Phys. Rev. A* **6**, 211–229 (1972).
- D. Vernhet, J. P. Rozet, K. Wohrer, L. Adoui, C. Stéphan, A. Cassimi, J. M. Ramillon, Excitation in swift heavy ion-atom collisions. *Nucl. Instrum. Methods Phys. Res., Sect. B* **107**, 71–78 (1996).
- J. Tabet, S. Eden, S. Feil, H. Abdoul-Carime, B. Farizon, M. Farizon, S. Ouaskit, T. D. Märk, Absolute total and partial cross sections for ionization of nucleobases by proton impact in the Bragg peak velocity range. *Phys. Rev. A* **82**, 022703 (2010).
- T. Jahnke, U. Hergenroth, B. Winter, R. Dörner, U. Fröhling, P. V. Demekhin, K. Gokhberg, L. S. Cederbaum, A. Ehresmann, A. Knie, A. Dreuw, Interatomic and intermolecular coulombic decay. *Chem. Rev.* **120**, 11295–11369 (2020).
- M. Barat, P. Roncin, Multiple electron capture by highly charged ions at keV energies. *J. Phys. B Atomic Mol. Phys.* **25**, 2205–2243 (1992).
- J. H. D. Eland, The dynamics of three-body dissociations of dications studied by the triple coincidence technique pepipico. *Mol. Phys.* **61**, 725–745 (1987).
- J. H. D. Eland, Dynamics of fragmentation reactions from peak shapes in multiparticle coincidence experiments. *Laser Chem.* **11**, 259–263 (1991).
- R. Flammini, M. Satta, E. Fainelli, L. Avaldi, Effect of the charge localization in the C⁺ – H⁺ fragmentation pathway of the ethyne dication. *Phys. Rev. A* **83**, 014501 (2011).

46. V. Bernigaud, O. Kamalou, A. Lawicki, M. Capron, R. Maisonnay, B. Manil, L. Maunoury, J. Rangama, P. Rousseau, J.-Y. Chesnel, L. Adoui, B. A. Huber, ARIBE: A low energy ion beam facility in Caen. *Publ. Astron. Obs. Belgrade* **84**, 83–86 (2008).
47. T. Bergen, X. Biquard, A. Brenac, F. Chandezon, B. A. Huber, D. Jalabert, H. Lebius, M. Maurel, E. Monnard, J. Opitz, A. Pesnelle, B. Pras, C. Ristori, J. C. Rocco, Multiply charged cluster ion crossed-beam apparatus: Multi-ionization of clusters by ion impact. *Rev. Sci. Instrum.* **70**, 3244–3253 (1999).
48. F. Chandezon, B. A. Huber, C. Ristori, A new-regime Wiley-McLaren time-of-flight mass spectrometer. *Rev. Sci. Instrum.* **65**, 3344–3353 (1994).
49. M. Capron, S. Díaz-Tendero, S. Maclot, A. Domaracka, E. Lattouf, A. Ławicki, R. Maisonnay, J. Y. Chesnel, A. Méry, J. C. Pouilly, J. Rangama, L. Adoui, F. Martín, M. Alcamí, P. Rousseau, B. A. Huber, A multicoincidence study of fragmentation dynamics in collision of γ -aminobutyric acid with low-energy ions. *Chem. Eur. J.* **18**, 9321–9332 (2012).
50. S. Maclot, R. Delaunay, D. G. Piekarski, A. Domaracka, B. A. Huber, L. Adoui, F. Martín, M. Alcamí, L. Avaldi, P. Bolognesi, S. Díaz-Tendero, P. Rousseau, Determination of energy-transfer distributions in ionizing ion-molecule collisions. *Phys. Rev. Lett.* **117**, 073201 (2016).
51. D. Curtis, Coincidence studies of doubly charged ions formed by 30.4 nm photoionization. *Int. J. Mass Spectrom. Ion Process.* **63**, 241–264 (1985).
52. K. Schäfer, W. Y. Baek, K. Förster, D. Gassen, W. Neuwirth, Analysis of initial energies of fragments produced by 65-keV proton-molecule collisions using a time-of-flight mass spectrometer. *Zeitschrift für Phys. D Atoms, Mol. Clusters* **21**, 137–143 (1991).
53. S. Tomita, H. Lebius, A. Brenac, F. Chandezon, B. A. Huber, Kinetic-energy release and fragment distribution of exploding, highly charged C_{60} molecules. *Phys. Rev. A* **65**, 053201 (2002).
54. T. H. Dunning Jr., Gaussian basis sets for use in correlated molecular calculations. I. The atoms boron through neon and hydrogen. *J. Chem. Phys.* **90**, 1007–1023 (1989).
55. T. Shiozaki, BAGEL: Brilliantly advanced general electronic-structure library. *WIREs Comput. Mol. Sci.* **8**, e1331 (2017).
56. I. Fdez. Galván, M. Vacher, A. Alavi, C. Angeli, F. Aquilante, J. Autschbach, J. J. Bao, S. I. Bokarev, N. A. Bogdanov, R. K. Carlson, L. F. Chibotaru, J. Creutzberg, N. Dattani, M. G. Delcey, S. S. Dong, A. Dreuw, L. Freitag, L. M. Frutos, L. Gagliardi, F. Gendron, A. Giussani, L. González, G. Grell, M. Guo, C. E. Hoyer, M. Johansson, S. Keller, S. Knecht, G. Kovačević, E. Källman, G. L. Manni, M. Lundberg, Y. Ma, S. Mai, J. P. Malhado, P. Å. Malmqvist, P. Marquetand, S. A. Mewes, J. Norell, M. Olivucci, M. Oppel, Q. M. Phung, K. Pierloot, F. Plasser, M. Reiher, A. M. Sand, I. Schapiro, P. Sharma, C. J. Stein, L. K. Sørensen, D. G. Truhlar, M. Ugandi, L. Ungur, A. Valentini, S. Vancouillie, V. Veryazov, O. Weser, T. A. Wesolowski, P.-O. Widmark, S. Wouters, A. Zech, J. P. Zobel, R. Lindh, OpenMolcas: From source code to insight. *J. Chem. Theory Comput.* **15**, 5925–5964 (2019).
57. M. Richter, P. Marquetand, J. González-Vázquez, I. Sola, L. González, SHARC: Ab initio molecular dynamics with surface hopping in the adiabatic representation including arbitrary couplings. *J. Chem. Theory Comput.* **7**, 1253–1258 (2011).
58. J. W. Park, R. Al-Saadon, N. E. Strand, T. Shiozaki, Imaginary shift in CASPT2 nuclear gradient and derivative coupling theory. *J. Chem. Theory Comput.* **15**, 4088–4098 (2019).

Acknowledgments: All calculations were performed at the MareNostrum Supercomputer of the Red Española de Supercomputación (BSC-RES) and the Centro de Computación Científica de la Universidad Autónoma de Madrid (CCC-UAM). The research was conducted in the framework of the International Associated Laboratory (LIA-CNRS) “Fragmentation dynamics of complex molecular systems-DYNAMO”. **Funding:** Work supported by the MICINN projects PID2019-105458RB-I00, PID2019-106732GB-I00, and PID2019-110091GB-I00, the “Severo Ochoa” Programme for Centres of Excellence in R&D (SEV-2016-0686), the “María de Maeztu” Programme for Units of Excellence in R&D (CEX2018-000805-M), and the European COST Actions CA18212 MD-GAS and CA18222 AttoChem. J.K. acknowledges support for a visit to GANIL, Caen (France) from the Polish Ministry of Science and Higher Education via statutory activity subsidy (no. 25/20/B). **Author contributions:** P.R., J.K., A.D., and B.A.H. designed and performed the experiments and analyzed the experimental data. J.G.-V., D.G.P., S.D.-T., and F.M. designed and performed the theoretical calculations and analyzed the theoretical data. All authors discussed the results. P.R., S.D.-T., and F.M. wrote the first version of the manuscript, and all authors contributed to their improvement. F.M. coordinated the project. **Competing interests:** The authors declare that they have no competing interests. **Data and materials availability:** All data needed to evaluate the conclusions in the paper are present in the paper and/or the Supplementary Materials.

Submitted 3 February 2021

Accepted 11 August 2021

Published 1 October 2021

10.1126/sciadv.abg9080

Citation: P. Rousseau, J. González-Vázquez, D. G. Piekarski, J. Kopyra, A. Domaracka, M. Alcamí, L. Adoui, B. A. Huber, S. Díaz-Tendero, F. Martín, Timing of charge migration in betaine by impact of fast atomic ions. *Sci. Adv.* **7**, eabg9080 (2021).

Timing of charge migration in betaine by impact of fast atomic ions

Patrick RousseauJesús González-VázquezDariusz G. PiekarskiJanina KopyraAlicja DomarackaManuel AlcamíLamri AdouiBernd A. HuberSergio Díaz-TenderoFernando Martín

Sci. Adv., 7 (40), eabg9080. • DOI: 10.1126/sciadv.abg9080

View the article online

<https://www.science.org/doi/10.1126/sciadv.abg9080>

Permissions

<https://www.science.org/help/reprints-and-permissions>

Use of this article is subject to the [Terms of service](#)

Science Advances (ISSN) is published by the American Association for the Advancement of Science. 1200 New York Avenue NW, Washington, DC 20005. The title *Science Advances* is a registered trademark of AAAS.
Copyright © 2021 The Authors, some rights reserved; exclusive licensee American Association for the Advancement of Science. No claim to original U.S. Government Works. Distributed under a Creative Commons Attribution NonCommercial License 4.0 (CC BY-NC).